Journal of Molecular Structure 1283 (2023) 135264

Contents lists available at ScienceDirect

Journal of Molecular Structure

journal homepage: www.elsevier.com/locate/molstr

Antioxidative limonoids from *Swietenia macrophylla* fruits: Experimental, DFT (Density Functional Theory) approach, and docking study

Phan Thi Thuy[a], Tran Trung Hieu[a], Dau Xuan Duc[a], Hoang Van Trung[b], Nguyen Huy Hung[c,d], William N. Setzer[e,f], Tran Dinh Thang[g], Ninh The Son[h,*]

[a] *Deparment of Chemistry, College of Education, Vinh University, 182 Le Duan, Vinh, Nghean, Vietnam*
[b] *School of Environmental Biochemistry Technology, Vinh University, 182 Le Duan, Vinh, Nghean, Vietnam*
[c] *Department of Pharmacy, Duy Tan University, 03 Quang Trung, Danang, Vietnam*
[d] *Center for Advanced Chemistry, Institute of Research and Development, Duy Tan University, Danang 550000, Vietnam*
[e] *Aromatic Plant Research Center, Lehi, UT 84043, United States*
[f] *Department of Chemistry, University of Alabama in Huntsville, Huntsville, AL 35899, United States*
[g] *Institute of Biotechnology and Food Technology, Industrial University of Ho Chi Minh City, Ho Chi Minh City, Vietnam*
[h] *Institute of Chemistry, Vietnam Academy of Science and Technology (VAST), 18 Hoang Quoc Viet, Cau Giay, Hanoi, Vietnam*

ARTICLE INFO

Article history:
Received 29 December 2022
Revised 12 February 2023
Accepted 28 February 2023
Available online 1 March 2023

Keywords:
Swietenia macrophylla
Limonoid
Antioxidant
Mosquito larvicidal
Density functional theory
Molecular docking

ABSTRACT

Phytochemical investigation of the methanol extract of *Swietenia macrophylla* fruit first led to the isolation of four limonoids seneganolide (**1**), khayanone (**2**), khayanolide B (**3**), and 6-acetoxy-methyl angolensate (**4**). Compound **3** (IC_{50} 3.18 μg/mL) was better than the positive control ascorbic acid (IC_{50} 7.18 μg/mL) in an antioxidative assay against DPPH (2,2-diphenyl-1-picrylhydrazyl) radicals. Compound **1** showed strong mosquito larvicidal activity against *Aedes aegypti* with LC_{50} values of 34.1–44.1 μg/mL and LC_{90} values of 57.3–65.1 μg/mL for 24 and 48-h exposures. Based on DFT (density functional theory)/B3LYP/6–311G(d,p) method, the SPL-ET (sequential proton loss-electron transfer) antioxidative mechanism is essential for compound **3** in polar solvents, while the HAT antioxidative route is appropriate in weak or non-polar mediums. Methine group at carbon C-6 of this compound exerted the lowest BDE (bond dissociation energy) values of 72.9–73.8 kcal/mol in both four studied mediums gas, benzene, methanol, and water. In the kinetic reactions with $HOO^{\bullet}$, $CH_3OO^{\bullet}$, and $^{\bullet}NO_2$ radicals, 6-CH also generated the lowest Gibbs free energy of activation $\Delta G^{\#}$ values of 14.5–24.2 kcal/mol and the highest rate constant K values of 6.068×10^{1}–1.75×10^{6} L/mol.s. A molecular docking (MD) analysis of seneganolide with relevant *Ae. aegypti* protein targets revealed AChR (acetylcholine receptor), ACE2 (angiotensin converting enzyme 2), and aaNAT (arylalkylamine *N*-acetyltransferase) to be potential targets of this compound.

1. Introduction

Swietenia macrophylla, also known as mahogany, is a woody species of the Meliaceae family. This plant is widely distributed in rain, semi-deciduous, and deciduous forests of America and South East Asia [1]. Traditionally, the parts of this plant were utilized at most. For instance, its seeds have been often used for leishmaniasis, abortion, hypertension, diabetes, and malaria treatments [2]. The mahogany timbers are also appropriate for furniture purposes [3].

Limonoids (tetranortriterpenoids) and flavonoids can be seen as characteristics of either mahogany or *Swietenia* plants [4]. Because of the immense pharmacological importance, it is recognized that this species has a variety of biomedical characters, such as antiviral, antibacterial, anticancer, antimalarial, anti-nociceptive, antidiarrheal, hypolipidemic, and anti-infective, especially in terms of antioxidative and antifeedant activities [5]. Swietemacrophyllanin, a new constituent of Indonesian mahogany, exerted the IC_{50} value of 56 μg/mL against DPPH (2,2-diphenyl-1-picrylhydrazyl) free radicals better than that of the positive control trolox (IC_{50} 81 μg/mL) [4]. The alcoholic extract of mahogany twigs has a good insecticidal susceptibility against polyphagous pest *Spodoptera frugiperda* [6].

In the current study, we wish to report the chromatographic separation, and the NMR structural elucidation of secondary

* Corresponding author.
E-mail address: yamantson@gmail.com (N.T. Son).

https://doi.org/10.1016/j.molstruc.2023.135264
0022-2860/

metabolites from *S. macrophylla*, collected from Vietnam. The obtained isolates were subjected to antioxidative and mosquito larvicidal assays. In addition, *In silico* approaches, including DFT calculation and molecular docking, were taken into consideration in structure-activity relationships.

2. Experimental

2.1. General experimental procedures

The NMR data were measured by a Bruker Avance-500 MHz machine, and chemical shifts were shown in ppm with the TMS (tetramethylsilane) as an internal reference. For chromatographic separation, silica gels (40–63 μm, China) were used, whereas the TLC (thin layer chromatography analysis was carried out using silica gel 60 F_{254} (Merck, Germany). The UV lamp (254 and 365 nm), and indicators (10% H_2SO_4 and vanillin) were used to visualize the TLC spots.

2.2. Plant material

The fruits of *S. macrophylla* were collected from Cat Tien National Park, Dongnai, Vietnam in 08/2017. The plant was identified by Dr Nguyen Quoc Binh, Vietnam National Museum of Nature, VAST. A voucher specimen SMF-2017 was deposited in Vinh University.

2.3. Extraction and isolation

The dried powders of *S. macrophylla* fruits were immersed with methanol (3 × 10 L) at 25 °C. The combined extracts were evaporated under decreased pressure, to give a crude methanol extract (318.0 g). This extract was then suspended in methanol-water (1:1, v/v), and partitioned with *n*-hexane and ethyl acetate. The obtained ethyl acetate extract (105.0 g) was chromatographed on silica gel column [*n*-hexane-ethyl acetate (100:1 to 1:1, v/v)], to yield 5 fractions SME1-SME5. The fraction SME4 was fractionated by silica gel chromatography column [*n*-hexane-ethyl acetate (25:1 to 2:1, v/v)], to afford 7 sub-fractions SME41-SME47. Compound **2** (13.0 mg) was purified from the sub-fraction SME43 by using silica gel chromatography column [*n*-hexane-ethyl acetate (15:1, v/v)]. In the meantime, compounds **1** (18.0 mg) and **3** (34.0 mg) were separated from the sub-fraction SME44 by using *n*-hexane-ethyl acetate (9:1, v/v). Finally, compound **4** (12.5 mg) was obtained from the fraction SME4 [dichloromethane-methanol (9:1, v/v)].

Seneganolide (1): White powder; m.p. 278–279 °C; ESI-MS: $C_{26}H_{31}O_8$, *m/z* 471.1 $[M + H]^+$; ^{1}H NMR ($CDCl_3$, 500 MHz, δ (ppm)): 1.03 (3H, s, H-18), 1.19 (3H, s, H-28), 1.32 (3H, s, H-29), 1.41 (1H, br t, 12.5 Hz, H-12α), 1.41 (1H, m, H-11β), 1.61 (1H, m, H-11α), 1.76 (1H, dd, 2.0, 11.0 Hz, H-12β), 1.87 (1H, dd, 7.0, 13.5 Hz, H-30β), 2.01 (1H, br d, 11.5 Hz, H-9), 2.20 (1H, td, 2.0, 13.5 Hz, H-30α), 2.27 (1H, dd, 2.0, 7.0 Hz, H-14), 2.32 (1H, dd, 10.5, 7.0 Hz, H-5), 2.56 (1H, dd, 7.0, 15.0 Hz, H-6β), 2.70 (1H, dd, 11.0, 15.0 Hz, H-6α), 2.78 (1H, dd, 2.0, 19.5 Hz, H-15α), 2.83 (1H, dd, 7.0, 19.5 Hz, H-15β), 2.84 (1H, dd, 7.0, 13.5 Hz, H-2), 4.21 (1H, d, 12.0 Hz, H-19β), 4.45 (d, 11.5 Hz, H-19α), 5.28 (1H, s, H-17), 6.33 (1H, t, 1.0 Hz, H-22), 7.40 (1H, d, 2.0 Hz, H-23), 7.40 (1H, brs, H-21); ^{13}C NMR ($CDCl_3$, 125 MHz, δ (ppm)): 19.6 (C-29), 20.8 (C-11), 22.4 (C-18), 23.8 (C-28), 27.5 (C-15), 29.5 (C-6), 31.4 (C-30), 34.9 (C-12), 35.3 (C-13), 38.5 (C-5) 44.7 (C-4), 44.7 (C-14), 46.8 (C-10), 53.0 (C-2), 61.2 (C-9) 74.1 (C-19), 78.1 (C-17), 80.1 (C-8), 107.5 (C-1), 109.6 (C-22), 120.7 (C-20), 140.9 (C-21), 143.1 (C-23), 170.6 (C-16), 174.1 (C-7), 213.5 (C-3).

Khayanone (2): White powder; m.p. 170–172 °C; ESI-MS: $C_{27}H_{35}O_9$, *m/z* 503.1 $[M + H]^+$; ^{1}H NMR ($CDCl_3$, 500 MHz, δ (ppm)): 0.99 (3H, s, H-18), 1.19 (1H, m, H11-β), 1.26 (1H, m, H-12β), 1.27 (3H, s, H-28), 1.28 (3H, s, H-29), 1.36 (3H, s, H-19), 1.75 (1H, dd, 2.0, 7.5 Hz, H-14), 1.72 (1H, m, H-12α), 1.82 (1H, m, H-11α), 1.87 (1H, dd, 5.0, 13.0 Hz, H-9), 2.36 (1H, ddd, 2.0, 9.5, 15.0 Hz, H-30α), 2.75 (1H, dd, 7.5, 19.0 Hz, H-15β), 2.78 (1H, m, H-5), 2.78 (1H, brs, 8-OH), 2.82 (1H, dd, 2.0, 19.0 Hz, H-15α), 2.89 (1H, brs, 6-OH), 3.13 (1H, d, 15.0 Hz, H-30β), 3.14 (1H, d, 9.0 Hz, H-2), 3.83 (3H, s, $COOCH_3$), 4.42 (1H, m, H-6), 5.60 (1H, s, H-17), 6.37 (1H, m, H-22), 7.43 (1H, t, 2.0 Hz, H-23), 7.45 (1H, brs, H-21); ^{13}C NMR ($CDCl_3$, 125 MHz, δ (ppm)): 22.6 (C-11), 23.8 (C-18), 23.8 (C-28), 25.5 (C-19), 26.7 (C-29), 27.1 (C-15), 35.0 (C-12), 35.4 (C-13), 39.0 (C-30), 46.0 (C-5), 50.2 (C-4), 50.2 (C-10), 51.1 (C-14), 53.0 ($COO\underline{C}H_3$), 54.3 (C-2), 61.2 (C-9), 70.7 (C-6), 72.9 (C-8), 76.8 (C-17), 109.8 (C-22), 120.9 (C-20), 141.1 (C-21), 143.1 (C-23), 171.2 (C-16), 175.5 (C-7), 213.1 (C-1), 214.2 (C-3).

Khayanolide B (3): White powder; m.p. 305–307 °C; ESI-MS: $C_{27}H_{35}O_{10}$, *m/z* 519.2 $[M + H]^+$; ^{1}H NMR ($CDCl_3$, 500 MHz, δ (ppm)): 0.96 (1H, m, H-12α), 1.07 (3H, s, H-28), 1.10 (3H, s, H-18), 1.20 (1H, s, H-19), 1.38 (1H, d, 11.5 Hz, H-29β), 1.77 (1H, m, H-11β), 1.85 (1H, m, H-12β), 1.86 (1H, m, H-11α), 1.89 (1H, d, 11.5 Hz, H-29α), 2.09 (1H, d, 8.0 Hz, H-9), 2.60 (1H, d, 9.5 Hz, H-30), 2.77 (1H, d, 19.0 Hz, H-15β), 3.06 (1H, d, 7.0 Hz, H-5), 3.16 (1H, d, 19.0 Hz, H-15a), 3.40 (1H, d, 7.0 Hz, H-3), 3.71 (3H, s, $COOCH_3$), 4.20 (1H, d, 7.0 Hz, H-6), 4.50 (1H, dd, 7.0, 9.0 Hz, H-2), 5.64 (1H, s, H-17), 6.42 (1H, m, H-22), 7.41 (1H, t, 2.0 Hz, H-23), 7.47 (1H, brs, H-21); ^{13}C NMR ($CDCl_3$, 125 MHz, δ (ppm)): 14.4 (C-18), 16.4 (C-11), 17.6 (C-19), 19.2 (C-28), 26.0 (C-12), 32.0 (C-15), 37.6 (C-13), 40.7 (C-5), 42.6 (C-4), 44.6 (C-29), 52.1 ($COO\underline{C}H_3$), 56.0 (C-9), 59.3 (C-10), 63.2 (C-30), 71.4 (C-6), 72.2 (C-2), 78.5 (C-3), 81.2 (C-17), 81.4 (C-14), 84.2 (C-1), 86.9 (C-8), 110.0 (C-22), 120.6 (C-20), 140.9 (C-21), 142.6 (C-23), 171.7 (C-16), 175.4 (C-7).

6-Acetoxy-methyl angolensate (4): White powder; m.p. 207–209 °C; ESI-MS: $C_{29}H_{37}O_9$, *m/z* 529.2 $[M + H]^+$; ^{1}H NMR (acetone-d_6, 500 MHz, δ (ppm)): 0.92 (1H, s, H-18), 1.06 (3H, s, H-29), 1.16 (3H, s, H-19), 1.47 (3H, s, H-28), 2.20 (3H, s, 6-$COOCH_3$), 2.28 (1H, dd, 3.0, 4.0 Hz, H-9), 3.02 (1H, s, H-5), 3.67 (1H, dd, 3.0, 5.5 Hz, H-1), 3.77 (3H, s, 7-$COOCH_3$), 5.10 (1H, s, H-30β), 5.29 (1H, s, H-30α), 5.57 (1H, s, H-17), 6.47 (1H, m, H-22), 7.55 (1H, m, H-23), 7.58 (1H, m, H-21); ^{13}C NMR (acetone-d_6, 125 MHz, δ (ppm): 14.3 (C-18), 20.9 (6-$OCO\underline{C}H_3$), 23.0 (C-19), 24.4 (C-29), 24.8 (C-11), 25.2 (C-28), 29.3 (C-12), 34.3 (C-15), 39.9 (C-2), 41.9 (C-13), 45.2 (C-10), 47.4 (C-5), 49.4 (C-4), 51.7 (C-9), 53.1 (7-$COO\underline{C}H_3$), 73.0 (C-6), 78.9 (C-1), 79.9 (C-17), 81.7 (C-14), 110.8 (C-22), 112.4 (C-30), 122.3 (C-20), 141.7 (C-21), 143.9 (C-23), 146.9 (C-8), 169.6 (C-16), 170.4 (6-$O\underline{C}OCH_3$), 171.7 (C-7), 211.1 (C-3).

2.4. Antioxidative assay

The antioxidative activity of four isolated limonoids **1–4** was based on their scavenging of DPPH free radicals [7]. Basically, their ability to donate hydrogen atoms was assessed using the decolorization of the methanol solution of DPPH. In the methanol solution, DPPH creates a violet or purple color that, in the presence of antioxidants, fades to varying colors of yellow [7]. DPPH (0.1 mM) was dissolved by methanol to form a solution, and 2.4 mL of this solution was then added to limonoid (1.6 mL) in methanol, to reach serial concentrations of 500, 100, 20, 4, and 0.8 μg/mL. After being vortexed, the reaction mixture was maintained in the dark for 25 min. At 517 nm, the absorbance of the reaction mixture was determined spectrophotometrically. Ascorbic acid was used as a positive control. The percent of DPPH radical scavenging was expressed by the following equation:

$$DPPH\ radical\ scavenging(\%) = [(OD_o - OD_1)/OD_o] \times 100 \quad (1)$$

Where OD_o stands for the absorbance of the control, and OD_1 stands for the absorbance of the tested compounds/standard. Each

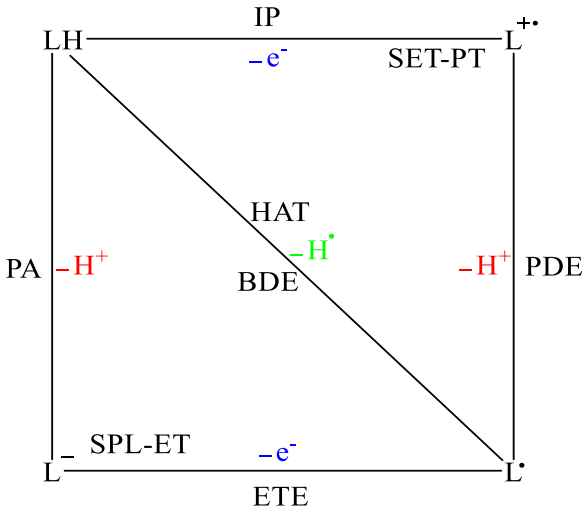

Fig. 1. The plausible antioxidative mechanisms.

experiment was repeated three times. The concentration was plotted against the percentage of inhibition, and the IC_{50} was determined from this graph.

2.5. Mosquito larvicidal assay

Aedes aegytpi mosquitoes were maintained at the Duy Tan University [8]. In dechlorinated water, mosquito eggs were born and fed with a 3:1 mixture of dog kibble and yeast. For the test, second-instar larvae were used. 25 Mosquito larvae were put into 15 mL glass vials with 4.0 mL of test solutions at doses of 100, 50, 25, 12.5 and 6.25 g/mL, with four replicates of each concentration. The tested limonoids **1–4** were dissolved in DMSO, and permethrin was used as a positive control. A solution containing 80 ml of DMSO was used as a negative control. Lethality data were evaluated by log-probit analysis to generate the LC_{50}, LC_{90}, and 95% confidence limits using Minitab® 19 (Minitab, LLC) after 24 and 48 h of exposure.

2.6. Computational methods

2.6.1. Antioxidative theory

The antioxidative calculation for compound **3** has been carried out using the Gaussian 09 package [9,10]. For the optimization of each compound's ionic and radical structures, the 6–311G(d,p) basis set was used in conjunction with the B3LYP (Becke, 3-parameter, Lee-Yang-Parr) functional. Both gas ($\varepsilon = 1$) and the solvents water ($\varepsilon = 78.39$), methanol ($\varepsilon = 32.63$), and benzene ($\varepsilon = 2.30$) have been used in the computations. The goal of frequency computation is to calculate frequencies that are accurate for zero-point energy (ZPE), which further proved that the ground states did not contain imaginary frequencies. The solvent impact was taken into account using the SCRF-PCM (self-consistent reaction field-polarizable continuum model).

Based on earlier studies [10,11], three renowned antioxidative mechanisms of a limonoid (LH) have been put forth: HAT (hydrogen atom transfer), SET-PT (single electron transfer-proton transfer), and SPL-ET (sequential proton loss-electron transfer) (Fig. 1).

The HAT is characterized by the BDE (bond dissociation energy). The IP (ionization potential) and the PDE (proton dissociation enthalpy) are responsible for the first and second steps of the SET-PT, respectively. Meanwhile, the PA (proton affinity) and the ETE (electron transfer enthalpy) are used to explain the first and second steps of the SPL-ET, respectively.

$$BDE = \Delta H(L^{\bullet}) + \Delta H(H^{\bullet}) - \Delta H(LH) \quad (2)$$

$$IP = \Delta H\left(L^{+\bullet}\right) + \Delta H\left(e^{-}\right) - \Delta H(LH) \quad (3)$$

$$PDE = \Delta H(L^{\bullet}) + \Delta H\left(H^{+}\right) - \Delta H\left(L^{\bullet+}\right) \quad (4)$$

$$PA = \Delta H\left(L^{-}\right) + \Delta H\left(H^{+}\right) - \Delta H(L) \quad (5)$$

$$ETE = \Delta H(L^{\bullet}) + \Delta H\left(e^{-}\right) - \Delta H\left(L^{-}\right) \quad (6)$$

The enthalpy ΔH of e^- and H^+ were extracted from similar reports [12]. At the same level, the TST (transition state theory) was used to consider the kinetic actions of compound **3** [10,11]. The rate constant K has a relation to $\Delta G^{\#}$ (Gibbs free energy of activation) by Eq. (7).

$$K(\mathrm{T}) = \kappa \frac{\mathrm{T}.k_{\mathrm{B}}}{h} \mathrm{e}^{\frac{-\Delta G^{\#}}{RT}} \quad (7)$$

Where κ is the Wigner coefficient, and h and k_B stand for the Plank and Boltzmann constants, respectively.

2.6.2. Molecular docking

The MD analysis of compound **1** was carried out as previously described [13]. Its chemical structure was assembled using Spartan 18 for Windows, v 1.4.4 (Wavefunction, Inc.). Molecular docking was carried out using Molegro Virtual Docker v 6.0.1 (Molegro ApS). A total of 10 relevant *Ae. aegypti* protein targets were used for molecular docking. Six protein targets were obtained from the Protein Data Bank (PDB): Arylalkylamine *N*-acetyltransferase, 4FD6, D7 salivary protein, 3DXL; glutathione *S*-transferase, 5FT3; odorant binding protein, 6OMW; and sterol carrier protein-2, 2QZT and 3BKS. In addition, four *Ae. aegypti* target proteins were prepared by homology modeling (see below): Acetylcholinesterase (AChE, based on PDB structures 1DX4 and 1QO9), acetylcholine receptor (AChR, based on 7EKP), and angiotensin-converting enzyme 2 (ACE2, based on 6S1Y). The orientations of the ligands with the target proteins were ranked based on the MolDock "rerank" energy values (E_{dock}).

Three-dimensional protein structures of *Ae. aegypti* AChE, AChR, and ACE2 are currently unavailable. Therefore, homology models were prepared using the SWISS-MODEL server (https://swissmodel.expasy.org). Appropriate protein target sequences were obtained from UniProt Knowledgebase (https://swissmodel.expasy.org). Three-dimensional structural models were obtained based on multiple-threading alignments, while the global model quality estimation was used to rank models (Table S1).

3. Results and discussion

3.1. Phytochemistry

Phytochemical study on the methanol extract of Vietnamese *S. macrophylla* fruits resulted in the isolation of four limonoids **1–4**. Based on NMR data analysis and comparison with literature, the chemical structures of these isolated limonoids were elucidated as seneganolide (**1**), khayanone (**2**), khayanolide B (**3**), and 6-acetoxymethyl angolensate (**4**) [14,15-17]. It noted that these compounds were found in *S. macrophylla* for the first time. The current result confirmed a close chemotaxonomic relationship between two genera *Swietenia* and *Khaya* since these isolates were found in various *Khaya* plants, especially *Khaya senegalensis*.

Table 1
The DPPH radical scavenging activity of compounds **1–4** and positive control ascorbic acid.

Concentration (μg/mL)	Inhibitory percentage				
	1	2	3	4	Ascorbic acid
500	8.64 ± 0.07	4.78 ± 0.40	90.1 ± 2.15	5.62 ± 0.32	99.71 ± 1.15
100	6.12 ± 0.26	3.40 ± 0.45	89.56 ± 3.13	2.73 ± 0.50	92.41 ± 3.26
20	2.18 ± 0.52	2.01 ± 0.30	89.22 ± 2.07	0.92 ± 0.84	80.48 ± 2.07
4	0	0	56.96 ± 4.51	0	27.61 ± 2.65
0.8	0	0	12.43 ± 1.44	0	18.43 ± 1.95
IC_{50} (μg/mL)	**> 500**	**> 500**	**3.18 ± 0.26**	**> 500**	**7.18 ± 0.67**

Table 2
Mosquito larvicidal activity against *Aedes aegypti* (μg/mL).

Sample 24-h treatment	LC_{50} (95% confidence levels)	LC_{90} (95% confidence levels)	χ^2	*p*
Compound **1**	44.1 (41.0218–47.1661)	65.1 (59.5487–73.8312)	0.085381	0.958
48-h treatment				
Compound **1**	34.1 (31.4243–37.0343)	57.3 (51.2597–66.4895)	4.24121	0.120

LC_{50}: 50% lethal concentration, LC_{90}: 90% lethal concentration, χ^2: Goodness-of-fit chi-square value and *p*: *p*-value.

3.2. Biological assessments

Four isolated limonoid derivatives **1–4** were subjected to antioxidative and mosquito larvicidal examinations, and the results are outlined in Tables 1-2. Regarding DPPH radical scavenging assay, khayanolide B (**3**) with the IC_{50} value of 3.18 ± 0.26 μg/mL was better than the positive control ascorbic acid (IC_{50} 7.18 ± 0.67 μg/mL). However, the remaining compounds were inactive (IC_{50} > 500 μg/mL). At the concentration of more than 20 μg/mL, DPPH radical scavenging percent of compound **3** reached up to 90%. As compared with literature compounds, the antioxidative activity of limonoid **3**, is also better than the new flavonoid swietemacrophyllanin (IC_{50} 56 μg/mL), and the other positive control trolox (IC_{50} 81 μg/mL) [4]. The ethanol extract of mahogany seeds also exhibited antioxidative potential in the model of streptozotocin-induced diabetic rats [5]. Collectively, it is recommended the use of mahogany constituents in the antioxidative treatment.

In the mosquito larvicidal assays, the first screening indicated that only limonoid seneganolide (**1**) showed activity (Table 2). Natural products exhibited strong mosquito repellent activity with $LC_{50} \leq 50$ μg/mL, moderate activity with $50 < LC_{50} \leq 100$ μg/mL, weak activity with $100 < LC_{50} \leq 750$ μg/mL, and inactive with $LC_{50} > 750$ μg/mL [8]. From Table 2, compound **1** showed strong mosquito larvicidal activity against *Ae. aegypti* with the 24-h LC_{50} value of 44.1 μg/mL, and the 24-h LC_{90} value of 65.1 μg/mL. For 48-h exposure, the LC_{50} and LC_{90} values were 34.1 and 57.3 μg/mL, respectively. Adhikari et al. reported that the petroleum ether extract of mahogany leaves strongly controlled the growth of 2nd larval mosquito *Culex quinquefasciatus* with the LC_{50} values of 33.45 and 29.37 μg/mL for 24 and 48-h treatments [18]. The methanol leaf extract caused 92.1% larval mortality towards *Ae. aegypti* [19]. It can be concluded that *Swietenia* constituents are appropriate for mosquito repellent activity. Based on this, we then moved on to the establishment of DFT-predictable calculation for antioxidative potential of khayanolide B (**3**) and molecular docking model for mosquito larvicidal activity of seneganolide (**1**).

3.3. Structural-electronic analyses

The optimized structure and FMO (frontier molecular orbital) analysis of compound **3** was carried out in four increasing polar media, gas, benzene, methanol, and water at B3LYP/6-311G(d,p) level. The optimized compound **3** includes a delocalization of the π-electrons in furan ring, a stable hydrogen bond between 3-OH and 2-O (1.922–1.295 Å) (Fig. 2 and Table S2). Hydroxy groups are flexible in space, whereas most methine/methylene protons are stable with axial and equatorial orientation. The dihedral angle θ_1(C13-C17-C20-C23) ranged from −103.47° to −96.61° in the four studied media (Table S2). The HOMO (highest occupied molecular orbital) distribution of **3** is again confirmed the stabilization of the furan unit (Fig. 2). The spin density represents a charge rate of an atom after H-abstraction, in which the lower spin density is in accordance with the lower BDE value (the better antioxidative activity) [20]. It is expected that 6-OH, and 8-OH, especially 1-OH, 6-CH, and 17-CH with the significant spin densities of 0.610–0.862 are good sites for antiradical reactions, whereas the remaining groups are accompanied by a spin density of more than 1.0 (Fig. 2). From Table S2, C–H bond distance of 6-CH and 17-CH groups are longer than those of 1-OH, 6-OH, and 8-OH groups. Hence, energies to break these two C–H bonds will be lower (the better antioxidant). Band gap energy ε_{gap} of compound **3** runs in a consistent order of gas (ε_{gap} = 5.654 eV) < benzene (ε_{gap} = 5.874 eV) < methanol (ε_{gap} = 6.129 eV) < water (ε_{gap} = 6.143 eV) (Table S2). It is expected that non-polar/weak polar media will facilitate reactions for saturated compounds such as limonoid **3**.

3.4. Antioxidative mechanisms

As can be seen, bond cleavage in the HAT mechanism is due to homolytic reaction. This process has been generally explained by the BDE value. The reaction BDE values of the good sites of compounds **3** were calculated at the B3LYP/6–311G(d,p) level (Table 3). In both four studied mediums, 6-CH group exerted the lowest BDE values of 72.9–73.8 kcal/mol, while the highest BDE values of 102.6–104.4 kcal/mol were assigned to 6-OH and 8-OH groups. In the meantime, the BDE values of 1-OH and 17-CH groups ranged from 83.9 to 85.7 kcal/mol. Another observation is that the BDE values of 1-OH, 6-CH, and 17-CH seem not to change, but the BDE values of 6-OH and 8-OH tend to slightly decrease when moved from the gaseous phase to solutions. To the best of our knowledge, this is the first time DFT calculations have been applied for limonoids. The obtained BDEs were comparable with those of well-known antioxidative, phenolic acids, benzofurans, or flavonoids [11,20,21].

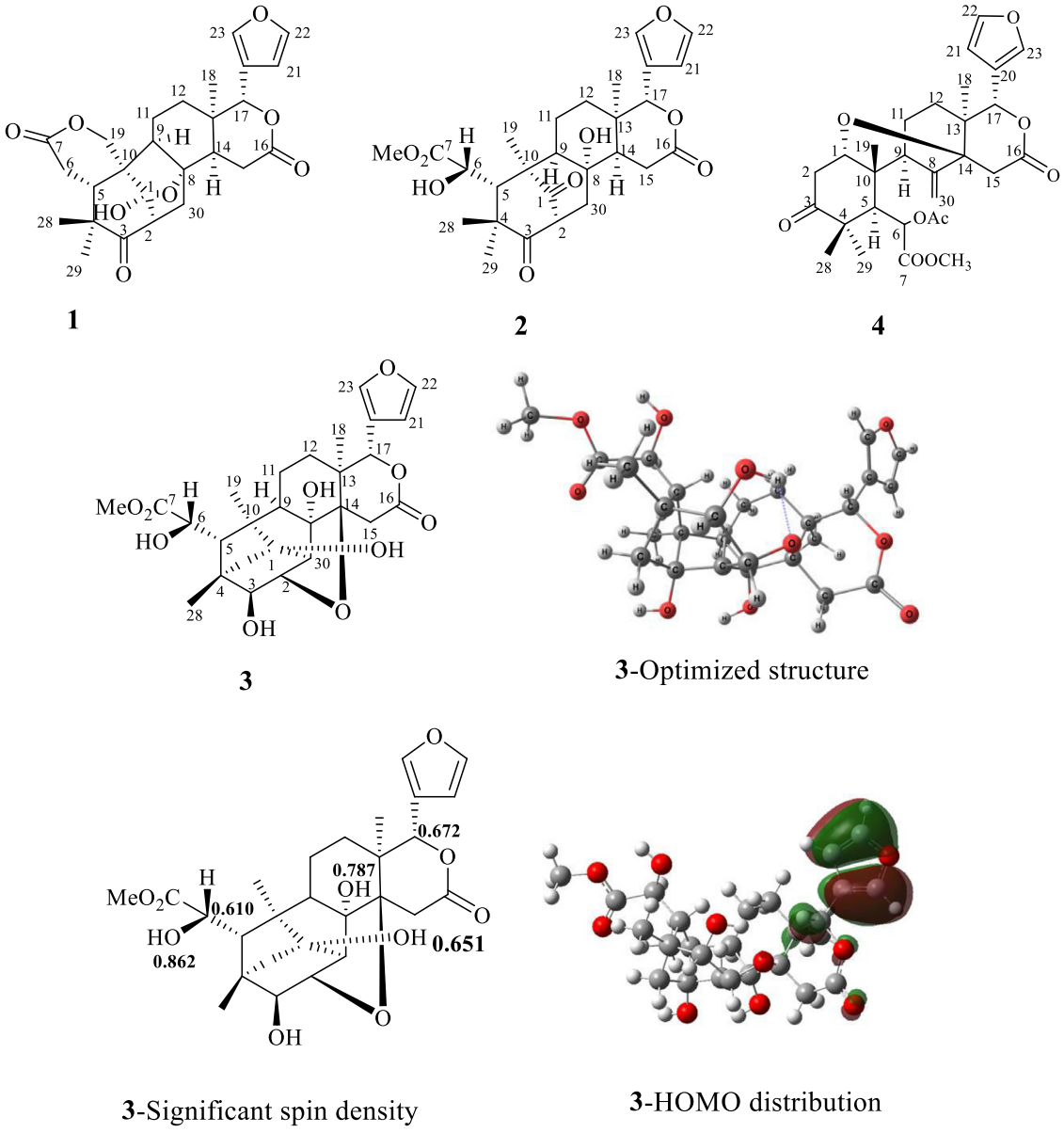

Fig. 2. Chemical structures of compounds **1–4**, and the optimized structure, significant spin density, and HOMO distribution of compound **3** at the B3LYP/6-311G(d,p) level.

Table 3
The reaction enthalpies of compound **3** at 298 K and the theoretical B3LYP/6-311G(d,p) level (kcal/mol).

No	BDE				IP				PDE			
	Gas	Benzene	CH_3OH	Water	Gas	Benzene	CH_3OH	Water	Gas	Benzene	CH_3OH	Water
1-OH	84.0	84.0	83.9	83.9	182	162	127	123	214.9	20.3	2.1	5.1
6-OH	104.4	104.2	103.6	103.7					236.8	42	23.3	26.4
8-OH	104.3	103.8	102.6	102.7					235.2	29.7	20.8	23.9
6-CH	72.9	73.3	73.8	73.8					205.3	11.1	6.5	3.5
17-CH	85.5	85.7	85.6	85.6					216.4	22	3.8	6.8

No	PA				ETE			
	Gas	Benzene	CH_3OH	Water	Gas	Benzene	CH_3OH	Water
1-OH	345.4	112.1	60.2	64.9	52.0	69.9	68.4	63.0
6-OH	359.5	124.5	70.1	74.2	59.8	79.2	80.6	75.0
8-OH	360.6	125.5	71.3	75.0	57.1	66.0	77.2	71.7
6-CH	352.7	120.7	69.3	73.3	35.0	52.1	48.7	45.9
17-CH	382.8	146.8	90.4	95.3	16.0	36.9	39.9	34.3

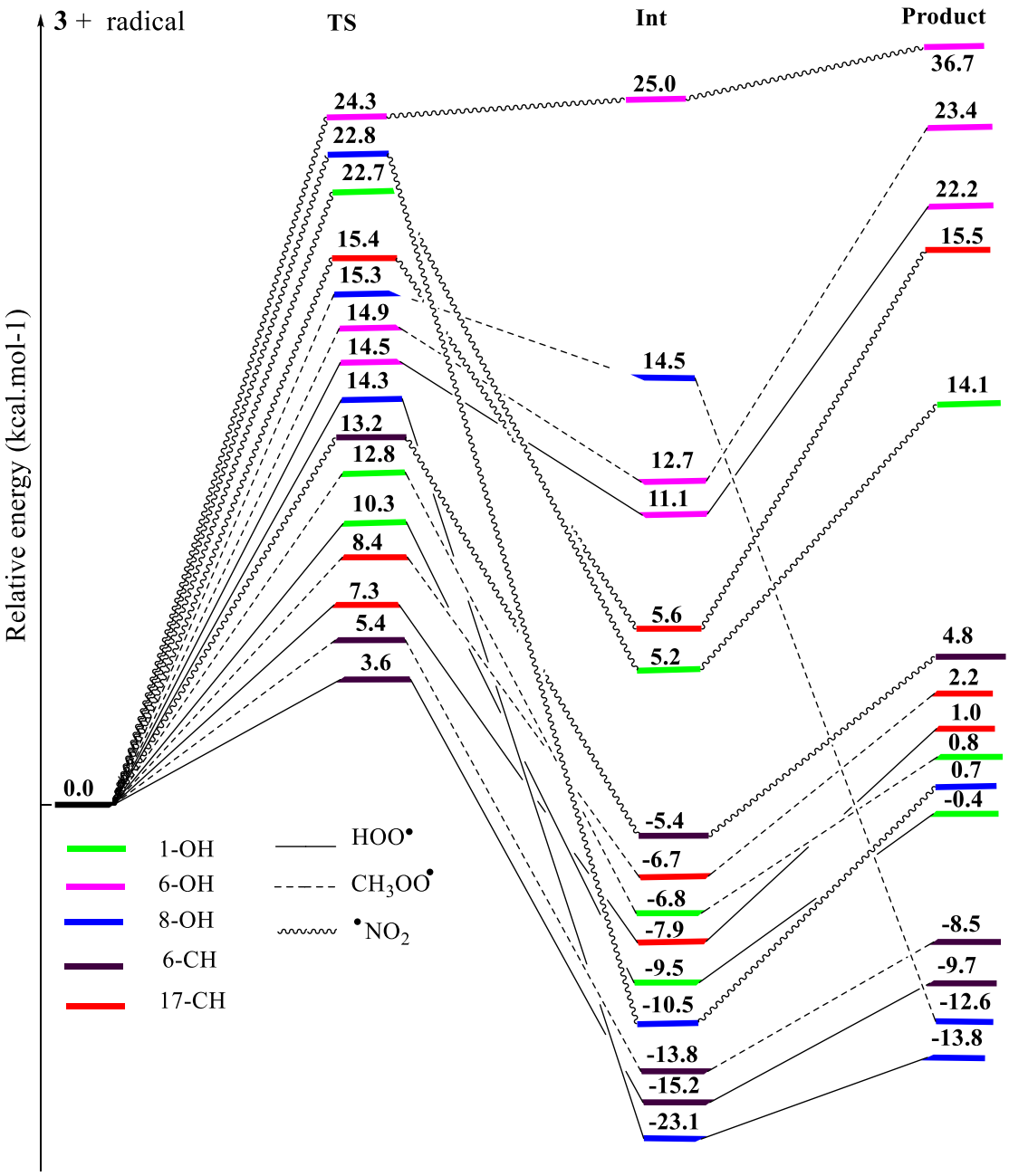

Fig. 3. Energy diagram for the reaction of $HOO^{\bullet}$, $CH_3OO^{\bullet}$ and $^{\bullet}NO_2$ radicals attack at the theoretical B3LYP/6-311G(d,p) level.

The first step of SET-PT is characterized by the IP calculation. As shown in Table 3, the IP values of limonoid **3** are much dependent on the change of environment, and they are found to run in order of gas > benzene > > methanol > water. It can be concluded that the electron loss from molecule LH to form radical cation $LH^{\bullet+}$ will be better in polar media. The second step of SET-PT is a heterolytic process, and is monitored by the PDE value. It is found that the gaseous PDE values are much greater than those in solvents, and an order for both two compounds is gas >> benzene > water > methanol. It reflects that a medium polar solvent, like methanol, would help to reduce the PDE energy. 1-OH and 17-CH are two best groups to possess the lowest methanolic PDE values of 2.8 and 3.8 kcal/mol, respectively. The next view is that the PDE values of 1-OH, 6-CH, and 17-CH are always better than those of 6-OH and 8-OH groups in each medium. This follows the same trend as the BDEs.

Taking the SPL-ET into consideration, 1-OH has induced the lowest PA value of 60.2 kcal/mol, whereas 17-CH causes the highest PA of 382.8 kcal/mol. It resembles the PDE values, the PA value of each group orderly run as gas >> benzene >> water > methanol. In each medium, the PAs also trend as 1-OH < 6-CH < 6-OH < 8-OH < 17-CH. The ETE energy represents electron transfer in the second step of the SPL-ET mechanism. The lowest ETE of 16 kcal/mol belongs to 17-CH in the gaseous phase. 6-OH is responsible for the highest ETE values of about 80 kcal/mol in benzene and methanol. Similar to the BDE values, and PDE values, the ETEs of 1-OH, 6-CH, and 17-CH are always lower than those of 6-OH and 8-OH in each medium. In each group, the gaseous ETE is always lower than that in solvents. It is argued that a non-polar medium like the gaseous phase is appropriate for electron transfer.

The preferential antioxidative mechanism for limonoid **3** is decided by the lowest BDE, IP, and PA enthalpies [10,20]. Generally,

Table 4
The gaseous $\Delta G^{\#}$ and K for $HOO^{\bullet}$, $CH_3OO^{\bullet}$ and $^{\bullet}NO_2$ radicals attack to compound **3** at the theoretical B3LYP/6-311G(d,p) level.

Position	$\Delta G^{\#}$ (kcal/mol) 3 + $HOO^{\bullet}$	K (L/mol.s)	$\Delta G^{\#}$ (kcal/mol) 3 + $CH_3OO^{\bullet}$	K (L/mol.s)	$\Delta G^{\#}$ (kcal/mol) 3 + $^{\bullet}NO_2$	K (L/mol.s)
1-OH	21.8	7.388×10^{2}	23.1	1.752×10^{2}	32.3	1.026×10^{-2}
6-OH	24.0	6.689×10^{1}	24.7	3.075×10^{1}	33.2	3.427×10^{-3}
8-OH	24.0	7.038×10^{1}	26.3	5.723	34.0	1.564×10^{-3}
6-CH	14.5	1.750×10^{6}	17.3	9.13×10^{4}	24.2	6.068×10^{1}
17-CH	18.8	1.890×10^{4}	20.6	2.834×10^{3}	26.8	3.852

Table 5
MolDock molecular docking scores (kJ/mol) for compound **1** with *Aedes aegypti* protein targets.

Compound	Protein targets									
	AChE (1DX4)[a]	AChE (1QO9)[a]	AChR (7EKP)[b]	ACE2 (6S1Y)[c]	aaNAT 4FD6	SCP2 2QZT	SCP2 3BKS	D7SP 3DXL	OBP 6OMW	GSTe2 5FT3
Seneganolide (**1**)	−14.1	−77.9	−106.3	−98.6	−95.8	−90.2	−79.3	−76.0	no dock	−35.4
Co-crystallized ligand	−110.8	none	−88.0	−100.9	none	−97.2	−102.8	−48.4	−104.5	−101.3

[a] The *Ae. aegypti* AChE protein structure is a homology model based on *Drosophila melanogaster* AChE.
[b] The *Ae. aegypti* AChR protein structure is a homology model based on human neuronal acetylcholine receptor subunit alpha-7.
[c] The *Ae. aegypti* ACE2 protein structure is a homology model based on *Anopheles gambiae* ACE2.

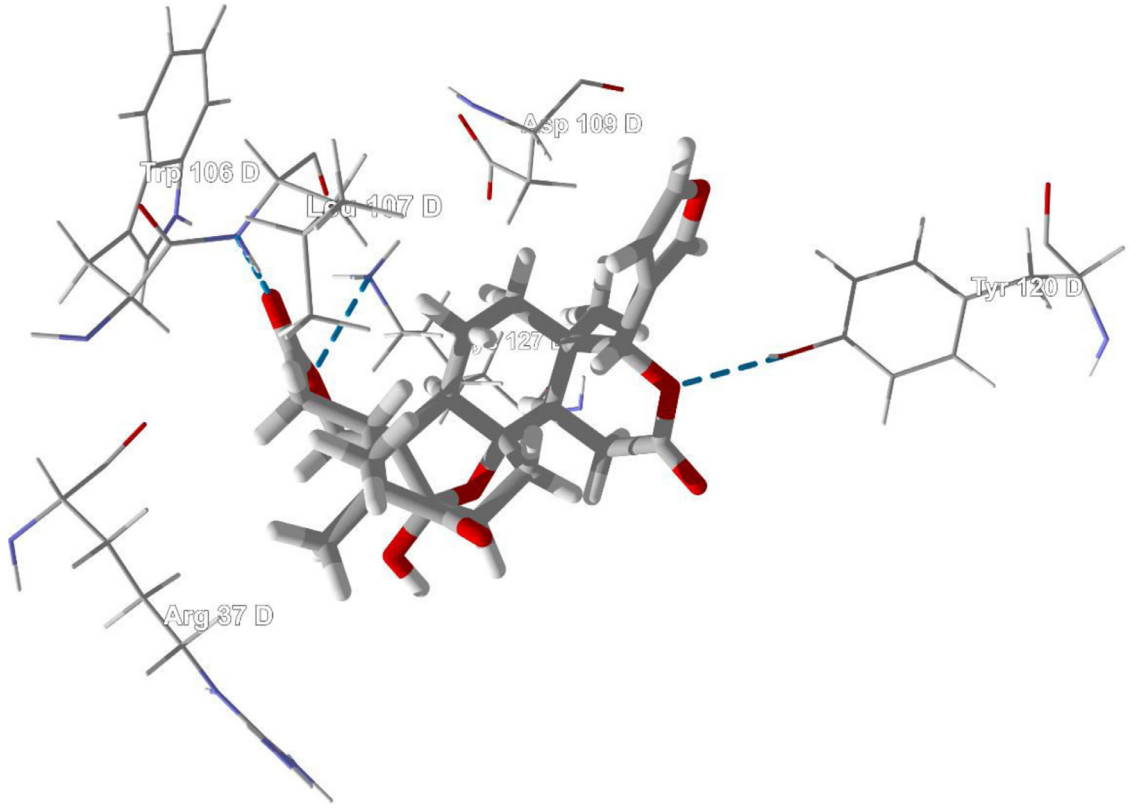

Fig. 4. Key intermolecular interactions of compound **1** and *Aedes aegypti* acetylcholine receptor (AChR). Hydrogen bonds are shown with a blue dashed line.

the PA values in methanol and water are lower than the BDE and IP values. As a consequence, the SPL-ET mechanism is essential for compound **3** in polar solvents. However, considering gas and benzene, it is viewed that the BDE values are less than the IP and PA values. Hence, the HAT seems to be the appropriate mechanism in weak or non-polar media.

3.5. Antioxidative kinetic actions

Reactive oxygen species (ROS), such as $ROO^{\bullet}$, have long been linked to the oxidative harm done to fatty acids, DNA, proteins, and other organs [22]. There have been plenty of diseases due to ROS overproduction. Cancer, diabetic, cardiovascular, and neurodegenerative diseases are representative pathologies that are linked to oxidative stress, which is caused by an imbalance between excessive ROS formation and limited antioxidant defenses [22]. In this section, we propose a kinetic model when the above OH and CH groups of compound **3** interacted with $HOO^{\bullet}$, $CH_3OO^{\bullet}$, and $^{\bullet}NO_2$ radicals. At the theoretical B3LYP/6-311G(d,p) level and the gaseous phase, the reactions have undergone one transition state (TS) and one intermediate (Int) (Table 3 and Figs. 3 and S9-S11). The rate constant K and the Gibbs free energy of activation $\Delta G^{\#}$ are two key elements to evaluate a kinetic reaction, by which a good reaction site will have the lowest $\Delta G^{\#}$ values and the highest K val-

ues [11]. It matches well with the above enthalpy calculation, 6-CH interacts with these three ROS radicals and induces the lowest $\Delta G^{\#}$ values of 14.5–24.2 kcal/mol and the highest K values of 10^1–10^6 L/mol.s (Table 4). It is also found that 6-CH + these studied ROS radicals generates the lowest relative energy ΔE values of 3.6–13.2 kcal/mol (Fig. 3). In contrast, the reactions of 6-OH and 8-OH with these radicals possess the high $\Delta G^{\#}$ values of 24.0–34.0 kcal/mol and the low K values of 10^{-3}–10^1 L/mol.s, as well as the high ΔE values of 14.5–24.3 kcal/mol (Table 4 and Fig. 3). Last but not least, the K and $\Delta G^{\#}$ values in each case of **3** + $HOO^{\bullet}$ are always better than those of **3** + $CH_3OO^{\bullet}$ and **3** + $^{\bullet}NO_2$ (Table 4). This reflects that limonoid **3** will have reaction rates with hydroperoxide radicals greater than acetyloxyl and nitrogen dioxide radicals.

3.6. Molecular docking

As we know, many biological processes depend on the bindings of molecule ligands to big protein targets. Modern structure-based drug design relies heavily on the correct prediction of the binding mechanisms between the ligand and protein (the docking problem). Various tools, such as the density-functional tight-binding (DFTB) or MD could give insight information and more accurate for a large calculated system [13,23,24]. In this section, the MD analysis was carried out with seneganolide (**1**) and eight potential *Ae. aegypti* protein targets: acetylcholinesterase (AChE), acetylcholine receptor (AChR), angiotensin-converting enzyme 2 (ACE2), arylalkylamine *N*-acetyltransferase (aaNAT), sterol carrier protein 2 (SCP2), D7 salivary protein (D7SP), odorant-binding protein (OBP), and glutathione *S*-transferase epsilon 2 (GSTe2). The docking scores are summarized in Table 5.

Compound **1** showed excellent docking to *Ae. aegypti* acetylcholine receptor with docking energies more exothermic than the co-crystallized ligand. Based on the docking to *Ae. aegypti* protein targets, AChR, ACE2, and aaNAT are the best targets, while AChE and OBP are very poor targets. Key intermolecular interactions between this limonoid and *Ae. aegypti* protein targets are summarized in Table S3.

In insects, nicotinic acetylcholine receptors can be blocked by neonicotinoid insecticides [25]. Thus, the acetylcholine receptor is a recognized target for mosquito control. A three-dimensional protein structure of *Ae. aegypti* AChR is not yet available. Therefore, a homology model was prepared based on the X-ray crystal structure of human $\alpha 7$ nicotinic acetylcholine receptor (PDB: 7EKP). Limonoid **1** showed notable docking to *Ae. aegypti* AChR. The important interactions between compound **1** and *Ae. aegypti* AChR protein are shown in Fig. 4. Hydrogen bonding interactions as well as van der Waals interactions are important in the binding of the ligands to the receptor. Based on the molecular docking analysis, *Ae. aegypti* AChR, ACE2, and/or aaNAT may be important biomolecular targets of *S. macrophylla* limonoids. Furthermore, seneganolide (**1**) is the most promising components for inhibition of these mosquito enzymes.

4. Conclusion

Chromatographic separation on the methanol extract of Vietnamese *S. macrophylla* fruit resulted in the isolation of four limonoids. Their chemical structures were elucidated by spectroscopic data, including seneganolide (**1**), khayanone (**2**), khayanolide B (**3**), and 6-acetoxy-methyl angolensate (**4**). Compound **3** is excellent to capture DPPH free radicals since its IC_{50} value of 3.18 μg/mL was lower than that of the positive control ascorbic acid (IC_{50} 7.18 μg/mL). Compound **1** strongly inhibited the larvae of *Ae. aegypti* with LC_{50} values of 34.1–44.1 μg/mL and LC_{90} values of 57.3–65.1 μg/mL for 24 and 48-h treatments. The DFT calculation aided by B3LYP/6–311G(d,p) level indicated that the SPL-ET route is essential antioxidative mechanism for compound **3** in protic solvents methanol and water, but the HAT route is a representative in non-polar/weak media gas and benzene. Hydroxy groups at carbons C-1, C-6, and C-8, methine group at carbon C-17, especially methine group at C-6 can be seen as good sites for antiradical reactions. 6-CH exerted the lowest BDE values of 72.9–73.8 kcal/mol in the four studied media. In addition, it possessed the lowest Gibbs free energy of activation $\Delta G^{\#}$ values of 14.5–24.2 kcal/mol and the highest rate constant K values of 6.068×10^1–1.75×10^6 L/mol.s in the kinetic reactions with ROS radicals $HOO^{\bullet}$, $CH_3OO^{\bullet}$, and $^{\bullet}NO_2$. The molecular docking analysis has shown acetylcholine receptor (AChR), angiotensin converting enzyme 2 (ACE2), and arylalkylamine *N*-acetyltransferase (aaNAT) to be potential targets of seneganolide. However, the proteomics of *Ae. aegypti* is not well established; there may be additional protein targets for this limonoid as well as non-protein targets.

Credit authorship contribution statement

Phan Thi Thuy: Project administration and DFT calculation, **Tran Trung Hieu**: Formal analysis, **Dau Xuan Duc**: Data curation, **Hoang Van Trung**: Methodology, **Nguyen Huy Hung**: Biological assay· **William N. Setzer**: Docking calculation, **Tran Dinh Thang**: Conceptualization, **Ninh The Son**: Formal analysis, writing and supervision

Funding

This work was financed by Vietnam Ministry of Education and Training, grant number B2021-TDV-07.

Declaration of Competing Interest

The authors declare that there is no conflict of interest.

Data availability

No data was used for the research described in the article.

Acknowledgements

All persons who have made substantial contributions to the work reported in the manuscript (e.g., technical help, writing and editing assistance, general support), but who do not meet the criteria for authorship, are named in the Acknowledgements and have given us their written permission to be named. If we have not included an Acknowledgements, then that indicates that we have not received substantial contributions from non-authors.

Supplementary materials

Supplementary material associated with this article can be found, in the online version, at doi:10.1016/j.molstruc.2023.135264.

References

[1] A.M.M. Eid, N.A. Elmarzugi, H.A. El-Enshasy, A review on the phytopharmacological effect of *Swietenia macrophylla*, Int. J. Pharm. Sci. 5 (2013) 47–53.
[2] G. Bourdy, S.J. DeWalt, C.D. Michel, A. Roca, V.M. Balderrama, C. Quenevo, A. Gimenez, Medicinal plants uses of the Tacana, an Amazonian Bolivian ethnic group, J. Ethnopharmacol. 70 (2000) 87–109.
[3] M.R. Lemes, R.P.V. Brondani, D. Grattapaglia, Multiplexed systems of microsatellite markers for genetic analysis of mahogany, *Swietinia macrophylla* king (Meliaceae), a threatened neotropical timber species, J. Hered. 93 (2002) 287–290.
[4] S. Falah, T. Suzuki, T. Katayama, Chemical consituents from Swietenia macrophylla bark and their antioxidant activity, Pak. J. Bio. Sci. 11 (2008) 2007–2012.

[5] S.Z. Moghadamtousi, B.H. Goh, C.K. Chan, T. Shabab, H.A. Kadir, Biological activities and phytochemicals of Swietenia macrophylla king, Molecules 18 (2013) 10465–10483.
[6] D. Alvarez, D. Zuleta, C. Saldamando, T. Lobo-Echeverri, Selective activity of *Carapa guianensis* and *Swietenia macrophylla* (Meliaceae) against the corn and rice strains of *Spodoptera frugiperda* (Lepidoptera, Noctuidae), Int. J. Pest. Manag. (2021), doi:10.1080/09670874.2021.1981484.
[7] A.I. Elshamy, T. Yoneyama, N.V. Trang, N.T. Son, Y. Okamoto, S. Ban, M. Noji, A. Umeyama, A new cerebroside from the entomopathogenic fungus *Ophiocordyceps longiissima*: structural-electronic and. antioxidant relations, experimental and DFT calculated studies, J. Mol. Struct. 1200 (2020) 127061.
[8] L.T. Huong, L.N. Sam, C.N. Giang, D.N. Dai, I.A. Ogunwande, Chemical composition and larvicidal activity of essential oil from rhizomes of *Amomum rubidium* growing in Vietnam, J. Essent. Oil. Bear. Plants 23 (2020) 405–413.
[9] N.T. Son, P.T. Thuy, N.V. Trang, Antioxidative capacities of stilbenoid suaveolensone A and suaveolensone B: a detailed analysis of structural-electronc properties and mechanisms, J. Mol. Struct. 1224 (2021) 129025.
[10] P.T. Thuy, N.V. Trang, N.T. Son, Antioxidant of 2-phenylbenzofuran derivatives: structural-electronic effects and mechanisms, RSC Adv. 10 (2020) 6315–6332.
[11] N.T. Son, D.T.M. Thanh, N.V. Trang, Flavone norartocarpetin and isoflavone 2′-hydroxygenistein: a spectroscopic study for structure, electronic property and antioxidant potential using DFT (Density functional theory), J. Mol. Struct. 1193 (2019) 76–88.
[12] M. Najafi, K.H. Mood, M. Zahedi, E. Klein, DFT/B3LYP study of the substituent effect on the reaction enthalpies of the individual steps of single electron transfer-proton transfer and sequential proton loss electron transfer mechanisms of chroman derivatives antioxidant action, Comput. Theor. Chem. 969 (2021) 1–12.
[13] M.S. Setzer, J. Sharifi-Rad, W.N. Setzer, The search for herbal antibiotics: an in-silico investigation of antibacterial phytochemicals, Antibiotics 5 (2016) 30.
[14] M. Nakatani, S.A.M. Abdelgaleil, H. Okamura, T. Iwagawa, A. Sato, M. Doe, Khayanolides A and B, new rearranged phragmalin limonoid antifeedants from *Khaya senegalensis*, Tetrahedron Lett. 41 (2000) 6473–6477.
[15] H. Zhang, D. VanDerveer, X. Wang, F. Chen, X.M. Androulakis, M.J. Wargovich, 6S,8a-dihydroxy-14,15-dihydrocarapin (Khayanone) from the stem bark of *Khaya senegalensis* (Meliaceae): isolation and its crystal structure, J. Chem. Crystallogr. 37 (2007) 463–467.
[16] S.A.M. Abdegaleil, H. Okamura, T. Iwagawa, A. Sato, I. Miyahara, M. Doe, M. Nakatani, Khayanolides, rearranged pharagmalin limonoid antifeedants from *Khaya senegalensis*, Tetrahedron 57 (2011) 119–126.
[17] V.T. Hien, V.D. Hoang, Chemical constituents of fruits of Khaya senegalensis A. Juss growing in Vietnam, Vietnam J. Chem. 54 (2016) 781–785.
[18] U. Adhikari, S. Singha, G. Chandra, In vitro repellent and larvicidal efficacy of *Swietenia mahagoni* against the larval froms of *Culex quinquefasciatus* Say, Asian Pac. J. Trop. Biomed. 2 (2012) S260–S264.
[19] P. Vasantha-Srinivasan, S. Karthi, R. Ganesan, S. Senthil-Nathan, P. Krutmuang, M. Chellappandian, N. Radhakrisnan, A. Ponsankar, K. Karthick, A. Nelofer, The efficacy of methanolic extract of Swietenia mahagoni Jacp. (Meliaceae) and a commercial insecticide against laboratory and field strains of *Aedes aegypti* (Linn.) and their impact on its predator *Toxorhnchites splendens*, Biocatal. Agric. Biotechnol. 31 (2021) 101915.
[20] P.T. Thuy, P.M. Quan, D.X. Duc, N.T. Son, The antioxidative potential of procyanidin B1: DFT (density functional theory) and docking approaches, J. Mol. Model. 28 (2022) 356.
[21] C. Giacomelli, F.D.S. Miranda, N.S. Goncalves, A. Spinelli, Antioxidant activity of phenolic and related compounds: a density functional theory study on the O-H bond dissociation enthalpy, Rex. Rep. 9 (2004) 263–269.
[22] B. Hulya, Reactive oxygen species, Crit. Care Med. 33 (2005) S498–S501.
[23] S.I. Allec, Y. Sun, J. Sun, C.A. Chang, B.M. Wong, Heterogenous CPU+GPU-enabled stimulations for DFTB molecular dynamics of large chemical and biological systems, J. Chem. Theory Comput. 15 (2019) 2807–2815.
[24] T. Yoshikawa, N. Komoto, Y. Nishimura, H. Nakai, GPU-accelarated large-scale excited-state simulation based on divide-and-conquer time-dependent density-functional tight-binding, J. Comput. Chem. 40 (2019) 2778–2786.
[25] A.K. Jones, M. Grauso, D.B. Sattelle, The nicotinic acetylcholine receptor gene family of the malaria mosquito, *Anopheles gambiae*, Genomics 85 (2005) 176–187.